

Know Your Step: Faster and Better Alignment for Flow Matching Models via Step-aware Advantages

Zhixiong Yue^{1,2}, Zixuan Ni², Feiyang Ye³, Jinshan Zhang^{1*}, Sheng Shen², Zhenpeng Mi²

¹Zhejiang University

²HiThink Research

³Southern University of Science and Technology

yuezhixiong915@gmail.com, nizixuan@myhexin.com, feiyang.ye.uts@gmail.com,
zhangjinshan@zju.edu.cn, shensheng2@myhexin.com, mizhenpeng@myhexin.com

Abstract

Recent advances in flow matching models, particularly with reinforcement learning (RL), have significantly enhanced human preference alignment in few-step text-to-image generators. However, existing RL-based approaches for flow matching models typically rely on numerous denoising steps, while suffering from sparse and imprecise reward signals that often lead to suboptimal alignment. To address these limitations, we propose Temperature-Annealed Few-step Sampling with Group Relative Policy Optimization (TAFS-GRPO), a novel framework for training flow matching text-to-image models into efficient few-step generators well aligned with human preferences. Our method iteratively injects adaptive temporal noise onto the results of one-step samples. By repeatedly annealing the model's sampled outputs, it introduces stochasticity into the sampling process while preserving the semantic integrity of each generated image. Moreover, its step-aware advantage integration mechanism combines the GRPO to avoid the need for the differentiable of reward function and provide dense and step-specific rewards for stable policy optimization. Extensive experiments demonstrate that TAFS-GRPO achieves strong performance in few-step text-to-image generation and significantly improves the alignment of generated images with human preferences. The code and models of this work will be available to facilitate further research.

1. Introduction

Flow matching models have recently emerged as a popular paradigm for Text-to-Image (T2I) generation, acclaimed for their simplicity and ability to produce high-quality images [1, 2, 5, 34]. However, the significant inference latency,

coupled with the escalating computational costs that grow with the scale of inference steps, presents a major obstacle to its effective application in real-world business scenarios. While techniques like quantization can accelerate inference, they often lead to a significant degradation in generation quality [16, 19, 41]. Recent advances in few-step distillation, especially reinforcement learning (RL) based approaches, aim to preserve quality while drastically reducing sampling steps [4, 21, 22, 35].

However, RL-based training approaches rely on efficient sampling to collect rewards, but flow matching models typically require numerous iterative denoising steps (e.g., 20 to 40 steps or more) to generate a single sample [18, 37]. This gives rise to two primary challenges.

First, the sequential nature of the generation process creates a significant computational bottleneck, severely limiting training efficiency and scalability [15, 39]. This inefficiency is particularly pronounced in online RL settings where numerous samples must be generated and evaluated in real-time during training [23, 24]. For example, RL-guided distillation methods [14, 21, 25] demand full-step sampling of the flow models to calculate the diffusion distillation loss while applying reward-guided distillation. Although reward-centric methods [4, 12, 22] eliminate the need for expensive diffusion distillation loss, it remains dependent on the complete denoising trajectory for reward computation. Furthermore, these methods rely on differentiable reward functions, limiting their applicability.

Second, the lengthy denoising steps of flow matching models leads to a sparse reward problem, as a meaningful reward signal is only available after the complete denoising trajectory [11, 42]. This sparsity makes it exceedingly difficult to discern which specific denoising step taken during the generation process positively contributes to the final alignment outcome. Consequently, policies across all timesteps receive the same terminal reward [18, 37]. This

*Corresponding author.



Figure 1. Qualitative comparison of generations from 28 sampling steps of Flux.1-dev, MixGRPO, and 8 sampling steps of Flux-Hyper, Reward-Instruct, and the proposed TAfs-GRPO. TAfs-GRPO demonstrates superior performance in semantics and aesthetics alignment with fewer sampling steps than the baseline Flux.1-dev.

uniform credit assignment based on sparse terminal rewards fails to accurately credit contributions of different denoising steps, resulting in inefficient exploration and suboptimal convergence [8]. These challenges underscore the need for continued research into novel RL distillation frameworks that can overcome the sampling inefficiency and credit assignment problems inherent in fine-tuning flow matching models for enhanced human preference alignment.

To kill two birds with one stone, this work introduces Temperature-Annealed Few-step Sampling with Group Relative Policy Optimization (TAfs-GRPO), which addresses the sampling inefficiency and sparse reward problem commonly observed in flow matching RL-based distillation frameworks. It contains two key components: **Temperature-Annealed Sampling** and **Step-aware Advantage Integration**. The temperature-annealed sampling combines one-step sampling with temporal-based noise injection. By adding adaptive noise at different temporal steps to the result of a one-step sample, the procedure repeatedly anneals the sampling outcome. This iterative roll-back mechanism not only introduces stochasticity into the sampling process but also produces the essential semantic information at each sample, which significantly alleviates the reward sparsity problem commonly observed in flow matching models. The step-aware advantage integration combines the GRPO-based RL strategy with temperature-annealed sampling outcomes. While avoiding the need for the reward function to be differentiable, this module eval-

uates the image produced at each annealing step within every sample trajectory. By assigning an advantage score to each sample output, the method substantially increases the amount of informative reward available at each sampling step and mitigates the negative effects of sparse rewards on GRPO. Because of this, TAfs-GRPO not only increases the sampling frequency achievable by RL-based methods on flow matching models and alleviates reward sparsity, but also stabilizes policy optimization in the few-step generation regime. The experiments in Section 4 demonstrate that, under the same training configuration, our method achieves faster convergence compared to Reward-Instruct [22], and consistently outperforms it across all image quality metrics at both 4-step and 8-step sampling. The contributions of this paper are summarized as follows:

- We first introduce temperature-annealed sampling to the GRPO training framework for flow matching models, leveraging the noise addition process to provide a stochastic environment for online RL.
- We propose a novel RL-based framework named TAfs-GRPO, which improves the sampling efficiency and addresses the sparse reward problem by the step-aware advantage integration mechanism while training.
- The TAfs-GRPO trained model achieves high-quality results with far fewer steps, significantly speeding up inference. The model maintains high performance across a wide range of sampling steps, providing flexibility for deployment under different latency constraints.

2. Related Work

2.1. Preference Alignment for T2I Models

The alignment of T2I models with human preferences has become a critical research direction to enhance the usability, safety, and aesthetic quality of generated content. A prominent line of work adapts Reinforcement Learning from Human Feedback (RLHF) for diffusion models. Early approaches like Direct Preference Optimization (DPO) [29] and its variants [17, 30, 40] applied policy gradient algorithms to optimize the denoising process based on reward scores. These methods often suffer from high computational cost and instability.

To address these limitations, Group-based RL methods like GRPO are proposed, which improve sample efficiency by computing advantages over a group of generated images within a single denoising trajectory. DanceGRPO [37] is highlighted as the first unified framework to adapt GRPO to visual generation, enabling its application across diverse generative paradigms (diffusion models and rectified flows), tasks (text-to-image, text-to-video, image-to-video), foundation models, and reward models. It leverages Stochastic Differential Equations (SDE) sampling to introduce randomness and addresses training instability, demonstrating substantial improvements on the human preference alignment task. Flow-GRPO [18] integrates online RL into flow matching models by recasting the original deterministic Ordinary Differential Equation (ODE) as an equivalent SDE, formulating the denoising process as a Markov decision process.

To mitigate the computational overhead of full-step sampling in these methods, MixGRPO [15] proposes a mixed ODE-SDE sampling strategy with a sliding window mechanism. TempFlow-GRPO [8] addresses the temporal uniformity assumption in previous GRPO methods by introducing a trajectory branching strategy for precise credit assignment, leading to more temporally-aware optimization. Pref-GRPO [31] fundamentally reformulates the optimization objective from absolute reward score maximization to pairwise preference fitting.

However, existing preference alignment methods have paid little attention to the few-step generation setting, leaving its training paradigm largely unexplored.

2.2. Few-step Distillation of T2I models

Recent advances in T2I model distillation have increasingly adopted trajectory-based methods to enable efficient few-step sampling. Methods such as Latent Consistency Models (LCM) [20] and SANA-Sprint [3] learn the solution trajectory of the probability flow ODE (PF-ODE) over reduced time intervals, enforcing self-consistency across steps to approximate the original denoising process with minimal inference steps.

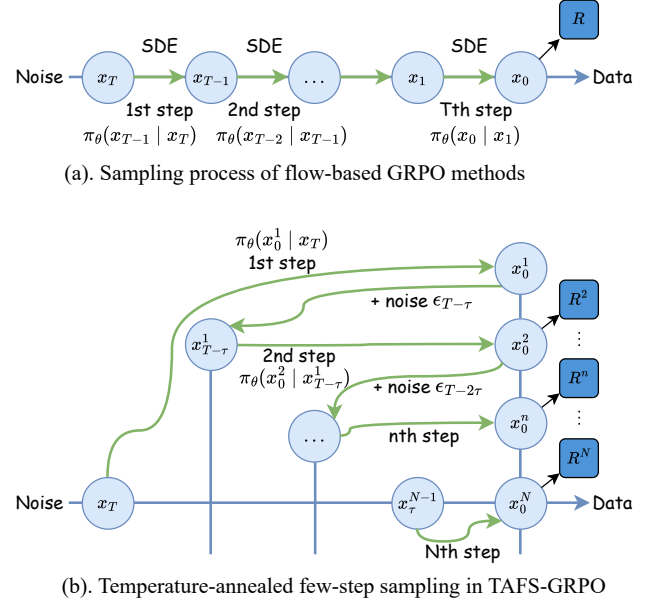


Figure 2. Comparison of sampling process between flow-based GRPO methods and TAFS-GRPO.

In contrast, distribution-based distillation aligns the student model’s generative distribution with that of the teacher model. This category includes GAN-based approaches like LADD [26], which employs adversarial training in latent space, and score distillation methods such as DMD [38] and its successor DMD2, which minimize distribution divergence without relying on instance-level trajectory matching.

Despite their effectiveness, these distillation techniques are often computationally intensive and typically depend on real image datasets. Recent efforts such as RG-LCD [14] and DI++ [21] incorporate reward maximization into the distillation process. However, they require training an additional score model to maintain proximity to the original generator, incurring substantial memory and computational overhead. LaSRO [12] addresses this by leveraging latent space surrogate rewards to optimize arbitrary reward signals through efficient off-policy exploration. Similarly, Reward-Instruct [22] observes that reward gradients dominate training, reducing diffusion distillation to a costly regularization role. It distills pre-trained diffusion models into reward-aligned few-step generators without distillation losses or training images. Nevertheless, this reward-centric approach still relies on differentiable reward functions, limiting its applicability and introducing computational inefficiency.

In comparison, TAFS-GRPO eliminates the need for differentiable reward functions by leveraging a policy gradient algorithm. Moreover, it introduces step-aware advantage integration mechanism to provide precise and dense evaluation feedback for the outcome of each stochastic sampling

action, which addresses the sparse reward problem.

3. Method

In this section, we first introduce the GRPO reinforcement learning method and discuss its insensitivity to the requirement of differentiability. Then we state the challenge of flow-based GRPO in the context of few-step fine-tuning. Finally, we propose TAFS-GRPO that leverages **Temperature-Annealed Sampling** and **Step-aware Advantage Integration** to address these challenges.

3.1. GRPO’s Robustness to Reward Objectives

The GRPO method has been widely applied in the field of natural language processing [7, 27]. Its main optimization objective $\mathcal{J}_{\text{GRPO}}(\theta)$ is defined as

$$\begin{aligned} \mathcal{J}_{\text{GRPO}}(\theta) = & \mathbb{E} \left[q \sim P(Q), \{o_i\}_{i=1}^G \sim \pi_{\theta_{\text{old}}}(O | q) \right] \\ & \frac{1}{G} \sum_{i=1}^G \frac{1}{|o_i|} \sum_{t=1}^{|o_i|} \left[\min Q_{i,t,\theta,\theta_{\text{old}}} - \beta \mathbb{D}_{KL} [\pi_{\theta} || \pi_{\text{ref}}] \right], \end{aligned} \quad (1)$$

where $Q_{i,t,\theta,\theta_{\text{old}}}$ can be formulated as:

$$Q_{i,t,\theta,\theta_{\text{old}}} = \min \left[r_{i,t,\theta,\theta_{\text{old}}} \hat{A}_{i,t}, \text{clip} (r_{i,t,\theta,\theta_{\text{old}}}, 1 - \varepsilon, 1 + \varepsilon) \hat{A}_{i,t} \right], \quad (2)$$

and $r_{i,t,\theta,\theta_{\text{old}}}$ is calculated by:

$$r_{i,t,\theta,\theta_{\text{old}}} = \frac{\pi_{\theta}(o_{i,t}|q, o_{i,<t})}{\pi_{\theta_{\text{old}}}(o_{i,t}|q, o_{i,<t})}. \quad (3)$$

Formally, for each question q sampled from the distribution $P(Q)$, a group of outputs $\{o_1, o_2, \dots, o_G\}$ are sampled from the old model $\pi_{\theta_{\text{old}}}$. $r_{i,t,\theta,\theta_{\text{old}}}$ is the important sample ratio between the probability of model π_{θ} and $\pi_{\theta_{\text{old}}}$ in each timestep t , where the policy models π_{θ} and $\pi_{\theta_{\text{old}}}$ are parameterized by θ and θ_{old} , respectively. The advantages $\hat{A}_{i,t}$ is a normalized reward of all $o_{i,<t}$, i.e., $\hat{A}_{i,t} = \tilde{r}_i = \frac{r_i - \text{mean}(\mathbf{r})}{\text{std}(\mathbf{r})}$. The policy model is optimized by maximizing the objective defined in Eq. (1).

In this process, the reward value r is derived from a pre-defined reward function R . However, this R is independent of the variables i , t , and o , and it does not participate in the gradient backpropagation of the objective function. As a result, in GRPO-based reinforcement learning, the reward function is not constrained to be continuous or differentiable. This property allows GRPO to effectively decouple the model optimization process from the specific formulation of the reward function, providing greater flexibility in designing task-specific rewards.

3.2. The Sparse Rewards of Flow-Based GRPO

While GRPO is compatible with a wide range of reward functions, it cannot be directly applied to an ODE-based

generation model. This arises because ODEs are deterministic: once we set the initial noise x_T , the entire sample trajectory x_t and the final output x_0 are predetermined. This determinism eliminates the inherent stochasticity that GRPO relies on for policy optimization.

To overcome this challenge, Flow-based GRPO reformulates the original ODE-based generation process as a SDE. This transformation introduces random noise during each sampling step at time t , enabling the model to generate samples of x_t and correspond to the output $o_{.,t}$. By incorporating this randomness, Flow-based GRPO can better capture the variability in the output over time. However, the intermediate result x_t generated during the denoising process lacks sufficient semantic information, which limits its utility for the reward function. The reward function R can only be applied to x_0 , as illustrated in the Figure 2(a). This constraint substantially diminishes the effectiveness of the reward function in guiding the flow-based GRPO model, as it disregards the influence of the context-dependent output $o_{.,t}$. Additionally, the need for multiple steps sampling to get one reward value r substantially increases both the training time and computational resource requirements for GRPO training.

3.3. Temperature-Annealed Few-step Sampling with GRPO

To address the challenges of sparse rewards and the high computational cost of multiple steps sampling, we propose Temperature-Annealed Few-step Sampling with GRPO. This approach is designed to introduce the necessary stochasticity for GRPO while dramatically improving training and inference efficiency. Our pipeline contains two key components: Temperature-Annealed Sampling and Step-aware Advantage Integration.

Temperature-Annealed Sampling. To mitigate the issue of reward signal discreteness inherent in the Flow-based GRPO method, we introduce a temperature-annealed sampling scheme. As illustrated in Figure 2(b), x_T is the Gaussian noise and x_0 is the final image. The T is the number of time steps of the Flow-based model v_{θ} . We set the total number of annealing steps to N , and uniformly divide the degradation interval into equal sub-sampling steps, each with a time increment of $\tau = T/N$. Starting from the initial noise x_T , we first perform a one-step sampling process to obtain the preliminary result x_0^1 with the velocity field $v_{\theta}(x_T, T)$ predicted by the flow model:

$$x_0^1 = T v_{\theta}(x_T, T), \quad (4)$$

And then, based on the remaining sampling steps $N - 1$, the strength of $T - \tau$ annealed noise $\epsilon_{T-\tau}$, which is constructed with noise scheduler of flow models [1, 5]. By interpolating between the sample x_0^1 and the degradation noise ϵ_0^1 , we

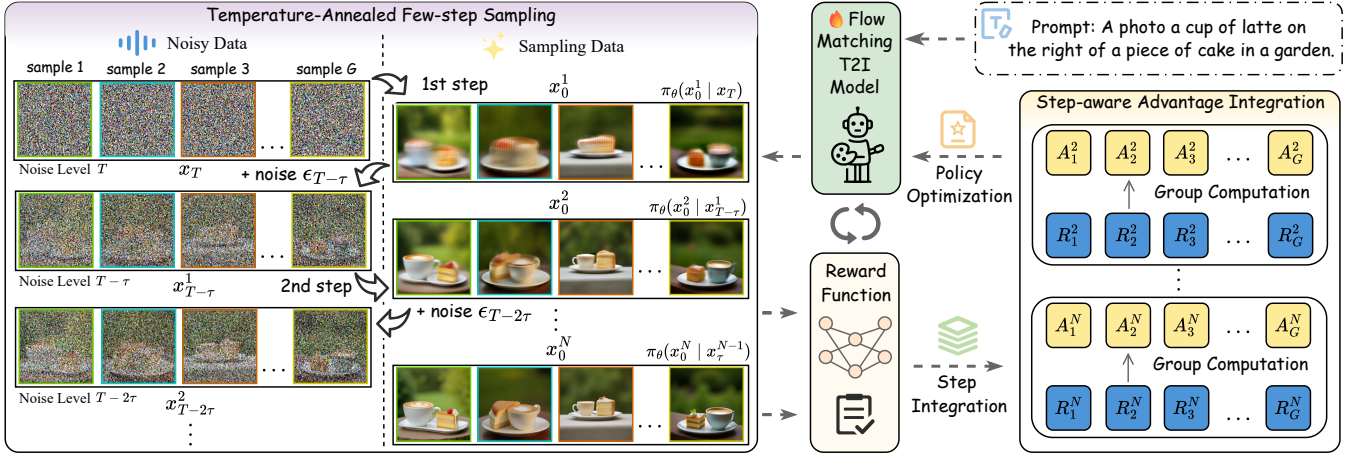


Figure 3. The architecture of the proposed TAFS-GRPO framework. Given a dataset of prompts, our temperature-annealed few-step sampling generates clean images in every sampling step. Then the step-aware advantage integration mechanism collects the rewards of these images and produces precise advantages of each sampling step. These precise feedback signals guide the few-step model updates.

construct a one-step annealed noisy sample $x_{T-\tau}$ by:

$$x_{T-\tau}^1 = x_0^1 + \epsilon_{T-\tau}, \quad (5)$$

Sampling from this distribution subsequently yields the corresponding state:

$$x_0^2 = x_{T-\tau}^1 + (T-\tau)v_\theta(x_{T-\tau}^1, T-\tau). \quad (6)$$

When repeating this process into annealing step $n+1$, the sampling result x_0^{n+1} can be written as:

$$x_0^{n+1} = x_0^n + \epsilon_{T-n\tau} + (T-n\tau)v_\theta(x_{T-n\tau}^n, T-n\tau). \quad (7)$$

where x_0^n is the sample from the annealing step n and $\epsilon_{T-n\tau}$ is the noise added at the annealing step $n+1$. The temperature-annealed sampling procedure not only introduces stochasticity into the sampling trajectory but also ensures that each intermediate sample retains meaningful semantic content.

Step-aware Advantage Integration. To mitigate the negative effects of sparse rewards and localize stochasticity to a single step, we propose a step-aware advantage integration mechanism to evaluate results with the same number of steps within a group. The advantages of the clean images denoised at different steps are then integrated to form the final evaluation.

Specifically, as shown in Figure 3, we first sample G distinct initial noise vectors $\{x_{T,i}\}_{i=1}^G$ from a normal distribution $\mathcal{N}(0, I)$. Since the first sampling step is deterministic, producing an initial set of clean images $\{x_{0,i}^1\}_{i=1}^G$, we bypass the evaluation on the results of the first step. We then inject G different noise vectors $\epsilon_{T-\tau}$ into these clean images to acquire the next noisy states $\{x_{T-1,i}^1\}_{i=1}^G$ for the second step. The second sampling step yields $\{x_{0,i}^2\}_{i=1}^G$,

Algorithm 1 TAFS-GRPO Training Process

Require: Prompt dataset \mathcal{C} , policy model π_θ , reward function \hat{R} , total sampling steps T , group size G

- 1: **for** training iteration $e = 1$ to E **do**
- 2: Update old policy: $\pi_{\theta_{\text{old}}} \leftarrow \pi_\theta$
- 3: Sample batch prompts $\mathcal{C}_b \sim \mathcal{C}$
- 4: **for** prompt $\mathbf{c} \in \mathcal{C}_b$ **do**
- 5: Initialize G noises $\{x_{T,i}\}_{i=1}^G \sim \mathcal{N}(0, I)$
- 6: **for** $n = N$ to 0 **do**
- 7: Sample a group: $\{x_{0,i}^n\}_{i=1}^G \sim \pi_{\theta_{\text{old}}}$
- 8: **if** $n > 1$ **then**
- 9: **for** each sample $i \in 1 \dots G$ **do**
- 10: Evaluate reward: $R_i^n \leftarrow \hat{R}(x_{0,i}^n, \mathbf{c})$
- 11: Integrate advantage: $A_i^n \leftarrow \frac{R_i^n - \mu_n}{\sigma_n}$
- 12: **end for**
- 13: **end if**
- 14: **if** $n < N$ **then**
- 15: Annealed noise $\epsilon_{T-n\tau}$: $\{x_{T-n\tau,i}^n\}_{i=1}^G$
- 16: **end if**
- 17: **end for**
- 18: $A_i \leftarrow \sum_{n=2}^N A_i^n$
- 19: **end for**
- 20: Compute GRPO loss $\mathcal{J}_{\text{policy}}(\theta)$
- 21: Update policy: gradient ascent on $\mathcal{J}_{\text{policy}}(\theta)$
- 22: **end for**

Ensure: Few-step policy model π_θ^*

which are evaluated by the reward function \hat{R} to get a group of rewards $\{R_i^2\}_{i=1}^G$.

We repeat this process to the n -th step, the step-specific rewards of the i -th sample is calculated by the reward func-

	Methods	NFE ↓	GenEval ↑	Pick Score ↑	CLIP ↑	HPS-v2.1 ↑	ImageR. ↑	Unified R. ↑
Pre-train	SD3.5-Medium [5]	40	67.99	22.95	28.70	0.285	0.947	3.496
	SD3.5-Large [5]	28	73.80	23.21	29.08	0.293	1.051	3.622
	Flux.1-dev [1]	28	67.54	23.41	28.19	0.305	1.013	3.562
	SANA-1.5 1.6B [34]	20	62.48	23.06	28.86	0.301	0.969	3.412
	HiDream-I1-Full [2]	50	80.46	23.47	28.84	0.325	1.334	3.748
Step-distillation	SD3.5-Large-Turbo [5]	4	69.62	23.18	28.90	0.287	0.927	3.522
	Flux.1-schnell [1]	4	67.82	23.01	28.61	0.295	0.918	3.538
	Flux-Turbo-Alpha [28]	4	61.41	23.06	27.57	0.290	0.837	3.404
	Hyper-Flux [25]	8	70.03	23.55	28.16	0.311	1.005	3.558
	SANA-Sprint 1.6B [3]	4	71.33	23.13	28.81	0.307	1.130	3.546
	HiDream-I1-Fast [2]	16	76.89	23.53	28.53	0.305	1.298	3.749
	TAFFS-GRPO+SD3.5M	4	80.84	22.61	30.03	0.274	1.052	3.598
	TAFFS-GRPO+SD3.5M	8	82.37	23.03	29.87	0.287	1.170	3.683
	TAFFS-GRPO+Flux	4	84.75	23.39	29.93	0.295	1.437	3.809
	TAFFS-GRPO+Flux	8	86.52	23.67	29.62	0.330	1.448	3.857

Table 1. Comprehensive comparison of TAFFS-GRPO with step distillation approaches in performance on the composition image generation task. ImageR. and Unified R. stand for ImageReward and Unified Reward. ↑ (↓) indicates the higher (lower) the result, the better the performance. We highlight the best and second best entries.

tion \hat{R} with prompt \mathbf{c} :

$$R_i^n = \hat{R}(x_{0,i}^n, \mathbf{c}), \quad (8)$$

The group-relative advantage $\{A_i^n\}_{i=1}^G$ is calculated by normalizing the rewards:

$$A_i^n = \frac{R_i^n - \mu_n}{\sigma_n}, \quad (9)$$

where μ_n and σ_n are the mean and variance of the rewards at step n for all samples within the group, respectively. In a total of N subsequent steps denoising for $\{x_{T,i}^n\}_{i=1}^G$, a group of final result images $\{x_{0,i}^N\}_{i=1}^G$ and the corresponding reverse-time trajectories $\{(x_{T,i}, x_{0,i}^1, \dots, x_{0,i}^N)\}_{i=1}^G$ are generated. Finally, the policy gradient loss function is formulated as:

$$\mathcal{J}_{\text{policy}}(\theta) = \frac{1}{G} \sum_{i=1}^G \frac{1}{N-1} \sum_{n=2}^N \left(\min \left(r_i^n(\theta) A_i^n, \text{clip} \left(r_i^n(\theta), 1 - \varepsilon, 1 + \varepsilon \right) A_i^n \right) \right), \quad (10)$$

where $r_i^n(\theta)$ is the probability ratio:

$$r_i^n(\theta) = \frac{p_{\theta} \left(x_{0,i}^n \mid x_{T-(n-1)\tau,i}^{n-1}, \mathbf{c} \right)}{p_{\theta_{\text{old}}} \left(x_{0,i}^n \mid x_{T-(n-1)\tau,i}^{n-1}, \mathbf{c} \right)}.$$

The detailed algorithm is illustrated in Algorithm 1.

4. Experiments

We conduct our experiments on two widely-used flow matching T2I base models, i.e., SD3.5-M [5] and Flux.1-dev [1], on the composition image generation task GenEval

[6] and the human preference alignment task pick-a-pic [13]. The composition image generation task assesses T2I models on complex compositional prompts, and the human preference alignment task aims to align T2I models with human preferences. These tasks empirically evaluate the ability of TAFFS-GRPO to distill and improve flow matching models.

4.1. Experimental Setup

We introduce two tasks and elaborate on their base models, training prompts, and reward metrics. For both tasks, we applied the Low-Rank Adaptation (LoRA) [10] method for text to image generation, following [15, 18, 37]. For the composition image generation task, we employ TAFFS-GRPO on both SD3.5-M and Flux.1-dev base models with a prompt dataset provided in GenEval following [18, 36]. For the human preference alignment task, we use Flux.1-dev as the base model. We perform experiments using the prompt provided by the Pick-a-Pic dataset [13] with 25432 text prompts for training and 2048 diverse text prompts for testing as suggested in [18, 36]. All methods are evaluated with 8 inference steps to ensure fairness.

Training Settings. We use the GenEval score, pick score, CLIP score and human preference score as the reward function in the training of the composition image generation task. We use the pick score and CLIP models as the in-domain reward models and evaluate both in-domain and out-of-domain (i.e., HPS-v2.1, Image Reward, and Unified Reward) metrics for the human preference alignment task. All methods are trained with 512 resolution. We utilize the AdamW optimizer with a learning rate of 3×10^{-4} and

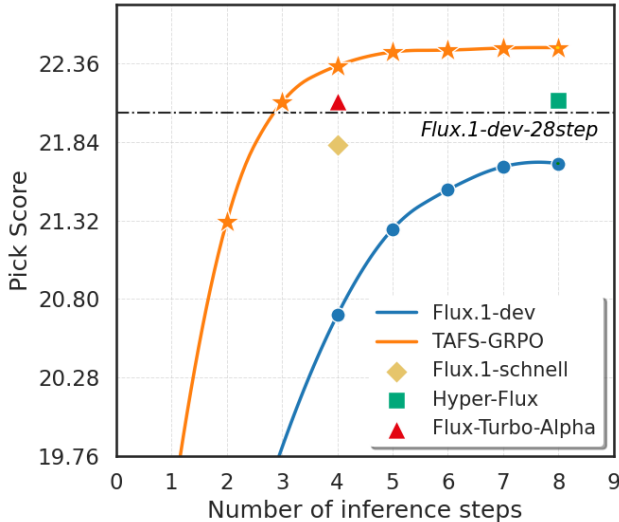


Figure 4. The pick score of various few-step model based on Flux.1-dev under different number of inference steps. TAFS-GRPO sustains high performance across 4 to 8 inference steps, illustrating its flexibility under different computational budgets.

weight decay of 1×10^{-4} for training with a group size of 48 and total batch size of 24.

Evaluation Metrics. For the composition image generation task, we use the GenEval score, pick score, CLIP score and human preference score as the reward function in training. We use the image reward and unified reward as the out-of-domain evaluation metrics. For the human preference alignment task, we use in-domain metrics, i.e., pick score and CLIP score, as the reward function during training and report both in-domain and out-of-domain metrics, i.e., human preference score, image reward, and unified reward in testing. All methods are evaluated with 1024 resolution.

4.2. Main Results

Composition Image Generation. Table 1 shows the results of TAFS-GRPO on the composition image generation task compared with various step distillation methods. Our TAFS-GRPO+Flux model not only surpasses other Flux-based step-distilled models, like Hyper-Flux (RL-guided step-distilled model) and Flux-Turbo-Alpha (distilled with extra data) on all metrics, but also outperforms larger models such as SD3.5-Large and HiDream-I1-Full. Our comparative study does not include DanceGRPO, MixGRPO, and Flow-GRPO because these methods do not employ step distillation techniques. We excluded RG-LCD and Reward-Instruct from our comparisons because these methods require the reward model to be differentiable. Our method achieves competitive results on both SD3.5-M and Flux, demonstrating its strong generalizability across different base models.

Human Preference Alignment. For the human preference

alignment task, we evaluated the computational overhead and performance of TAFS-GRPO compared to flow-based GRPO methods [15, 18, 37] and RL-based distillation methods [14, 22], with the results presented in Table 2. Compared to Flow-GRPO, TAFS-GRPO achieves significant improvements in various out-of-domain metrics under the same number of inference steps, while also increasing training speed by 53.2%. This demonstrates that temperature-annealed few-step sampling effectively enhances training efficiency. Due to the expensive distillation loss, RG-LCD trains significantly slower than TAFS-GRPO and Reward-Instruct. TAFS-GRPO achieves a relative improvement of 24.7% on HPS-v2.1 compared to RG-LCD, achieving superior alignment with human preferences. This indicates that step-aware advantage integration yields precise reward signals to enhance the optimization of the distillation model. Our approach delivers robust performance on the tasks of compositional image generation and human preference alignment, showing that it generalizes effectively to diverse tasks and datasets.

Visual Comparison. Figure 1 visualizes the result for the qualitative comparison with multiple prompts. With fewer NFE steps, the results of 8 NFE TAFS-GRPO show better semantic alignment than the results of 28 NFE FLUX.1-Dev, showing the effectiveness of TAFS-GRPO in distilling and improving the pre-trained flow matching model. Additionally, under the same 8 NFE, the results of TAFS-GRPO show richer details and better aesthetics compared with Reward-Instruct. The result of TAFS-GRPO reduces reward hacking compared to MixGRPO, which indicates the step-aware advantage integration precisely guides the early denoising steps, thereby mitigating the over-reliance on final-step rewards that drives the phenomenon.

Flexibility of the Inference Step. As shown in Figure 4, the TAFS-GRPO trained model achieves high-quality results with far fewer steps, significantly speeding up inference. The model maintains high performance across a wide range of sampling steps (i.e., 5-8), providing flexibility for deployment under different latency constraints. Compared with other Flux-based distilled models (i.e., Hyper-Flux [25], Flux-Turbo-Alpha [28] and Flux.1-schnell [1]), the TAFS-GRPO distilled model shows superior performance under different numbers of inference steps. The consistent performance maintenance across varying step counts (5-8 steps) demonstrates the efficacy of our step-aware advantage integration strategy. Our method achieves optimal trade-offs between computational efficiency and generation quality, effectively addressing the core challenge in few-step diffusion sampling.

4.3. Ablation Studies

To validate the effectiveness of TAFS-GRPO, we perform ablation studies on both the temperature-annealed few-step

Method	NFE $_{\pi_{\theta_{\text{old}}}}$ / NFE $_{\pi_{\theta}}$	Iteration Time (s) \downarrow	In-Domain		Out-of-Domain		
			Pick Score \uparrow	CLIP Score \uparrow	HPS-v2.1 \uparrow	ImageR. \uparrow	Unified R. \uparrow
Flux.1-dev [1]	-	-	21.68	25.95	0.280	0.848	3.328
DanceGRPO [37]	25 / 14	646	22.20	27.42	0.333	1.212	3.484
MixGRPO [15]	25 / 4	334	22.23	27.67	0.324	1.210	3.472
Flow-GRPO [18]	10 / 6	248	22.26	27.72	0.304	1.035	3.460
RG-LCD [14]	-	466	21.97	26.98	0.283	0.929	3.336
Reward-Instruct [22]	-	206	22.13	27.23	0.286	0.973	3.392
TAFS-GRPO	4 / 3	116	22.46	27.68	0.353	1.595	3.511

Table 2. Comparison of sampling efficiency and in-domain and out-of-domain performance on the human preference alignment task. ImageR. and Unified R. stand for ImageReward and Unified Reward. \uparrow (\downarrow) indicates that the higher (lower) the result, the better the performance. The number of Function Evaluations (NFE) and the time consumption per iteration with the same number of samples are used for the evaluation of computational overhead. NFE $_{\pi_{\theta_{\text{old}}}}$ and NFE $_{\pi_{\theta}}$ represent the number of forward propagations of the reference model and policy model for computing the policy ratio. We highlight the best entries.

sampling and the step-aware advantage integration mechanism, as shown in Table 3. For the “w/o MCS” variant, we replace the temperature-annealed sampling in the TAFS-GRPO method with the same number of SDE sampling steps. Compared with the original TAFS-GRPO methods, the performance of this variant degrades on both in-domain and out-of-domain metrics, which verifies the usefulness of the temperature-annealed few-step sampling. For the “w/o Step Adv.” variant, we replace the step-aware advantage integration with simply computing the group advantage of the final image rewards. This variant without the reward signal for each sampling step has inferior performance to the TAFS-GRPO method, which indicates that step-aware advantage integration can effectively improve the performance of the TAFS-GRPO method.

Method	Pick Score \uparrow	CLIP Score \uparrow	HPS-v2.1 \uparrow
TAFS-GRPO	22.46	27.68	0.353
- w/o TAFS	22.19	26.14	0.301
- w/o Step Adv.	21.77	24.60	0.288

Table 3. Ablation Study on the component of TAFS-GRPO. TAFS stands for the proposed temperature-annealed few-step sampling method. Step Adv. stands for the step-aware advantage integration mechanism.

As shown in Table 4, the performance of TAFS-GRPO constantly improves with the number of temperature-annealed steps increases, which validates the efficacy of the proposed framework. To balance training speed with performance, we select 3 temperature-annealed steps for the experiments.

To validate the effectiveness of step-aware advantage integration, we perform ablation studies on various numbers of advantage integration steps shown in Table 5. The performance of TAFS-GRPO shows consistent improvement with an increasing number of advantage integration steps,

N _{Annealed}	Time \downarrow	Pick Score \uparrow	CLIP Score \uparrow	HPS-v2.1 \uparrow
1	47	21.76	27.14	0.296
3	116	22.46	27.68	0.353
5	185	22.53	27.31	0.363

Table 4. Ablation study on the number of sampling steps in TAFS-GRPO Training. The Time column denotes the time consumption in seconds per training iteration.

providing compelling evidence that the step-aware advantage integration successfully directs reward signals to precisely optimize the model. As indicated in the Time column, the step-aware advantage integration introduces minimal computational overhead and does not significantly increase training time.

N _{Adv.}	Time \downarrow	Pick Score \uparrow	CLIP Score \uparrow	HPS-v2.1 \uparrow
1	107	21.77	24.60	0.288
2	112	22.02	26.17	0.301
3	116	22.46	27.68	0.353

Table 5. Ablation study on the number of advantage integration steps in TAFS-GRPO Training. N_{Adv.} stands for number of sampling step used for advantage integration. The number of temperature-annealed sampling steps is set to 3. The Time column denotes the time consumption in seconds per training iteration.

5. Conclusion

In this paper, we propose TAFS-GRPO, a method designed for efficient few-step training of flow-matching T2I models. We highlight the challenge of sampling efficiency and sparse reward when training flow matching models with RL. By integrating temperature-annealed few-step sampling into the GRPO framework, our approach substantially improves sampling efficiency, which is a critical factor for online RL methods. To mitigate the sparse reward issue,

we introduce a step-aware advantage integration mechanism, delivering more precise evaluation signals. As a result, TAFS-GRPO achieves accelerated few-step training on various flow matching models while enhancing alignment with human preferences on various prompt datasets and tasks. Notably, the few-step model trained by a single TAFS-GRPO process demonstrates robust performance across a wide range of sampling steps, offering flexibility for deployment under diverse latency constraints.

References

[1] Black Forest Labs. Flux, 2024. Accessed: 2024-09-04. [1](#), [4](#), [6](#), [7](#), [8](#)

[2] Qi Cai, Yehao Li, Yingwei Pan, Ting Yao, and Tao Mei. Hidream-i1: An open-source high-efficient image generative foundation model. In *Proceedings of the 33rd ACM International Conference on Multimedia*, pages 13636–13639, 2025. [1](#), [6](#)

[3] Junsong Chen, Shuchen Xue, Yuyang Zhao, Jincheng Yu, Sayak Paul, Junyu Chen, Han Cai, Song Han, and Enze Xie. Sana-sprint: One-step diffusion with continuous-time consistency distillation. *arXiv preprint arXiv:2503.09641*, 2025. [3](#), [6](#)

[4] Kevin Clark, Paul Vicol, Kevin Swersky, and David J Fleet. Directly fine-tuning diffusion models on differentiable rewards. *arXiv preprint arXiv:2309.17400*, 2023. [1](#)

[5] Patrick Esser, Sumith Kulal, Andreas Blattmann, Rahim Entezari, Jonas Müller, Harry Saini, Yam Levi, Dominik Lorenz, Axel Sauer, Frederic Boesel, et al. Scaling rectified flow transformers for high-resolution image synthesis. In *Forty-first international conference on machine learning*, 2024. [1](#), [4](#), [6](#)

[6] Dhruba Ghosh, Hannaneh Hajishirzi, and Ludwig Schmidt. Geneval: An object-focused framework for evaluating text-to-image alignment. *Advances in Neural Information Processing Systems*, 36:52132–52152, 2023. [6](#), [1](#)

[7] Daya Guo, Dejian Yang, Haowei Zhang, Junxiao Song, Ruoyu Zhang, Runxin Xu, Qihao Zhu, Shirong Ma, Peiyi Wang, Xiao Bi, et al. Deepseek-r1: Incentivizing reasoning capability in llms via reinforcement learning. *arXiv preprint arXiv:2501.12948*, 2025. [4](#)

[8] Xiaoxuan He, Siming Fu, Yuke Zhao, Wanli Li, Jian Yang, Dacheng Yin, Fengyun Rao, and Bo Zhang. Tempflow-grpo: When timing matters for grpo in flow models. *arXiv preprint arXiv:2508.04324*, 2025. [2](#), [3](#)

[9] Jack Hessel, Ari Holtzman, Maxwell Forbes, Ronan Le Bras, and Yejin Choi. Clipscore: A reference-free evaluation metric for image captioning. In *Proceedings of the 2021 conference on empirical methods in natural language processing*, pages 7514–7528, 2021. [1](#)

[10] Edward J Hu, Yelong Shen, Phillip Wallis, Zeyuan Allen-Zhu, Yuanzhi Li, Shean Wang, Lu Wang, Weizhu Chen, et al. Lora: Low-rank adaptation of large language models. *ICLR*, 1(2):3, 2022. [6](#)

[11] Zijing Hu, Fengda Zhang, Long Chen, Kun Kuang, Jiahui Li, Kaifeng Gao, Jun Xiao, Xin Wang, and Wenwu Zhu. Towards better alignment: Training diffusion models with reinforcement learning against sparse rewards. In *Proceedings of the Computer Vision and Pattern Recognition Conference*, pages 23604–23614, 2025. [1](#)

[12] Zhiwei Jia, Yuesong Nan, Huixi Zhao, and Gengdai Liu. Reward fine-tuning two-step diffusion models via learning differentiable latent-space surrogate reward. In *Proceedings of the Computer Vision and Pattern Recognition Conference*, pages 12912–12922, 2025. [1](#), [3](#)

[13] Yuval Kirstain, Adam Polyak, Uriel Singer, Shahbuland Matiana, Joe Penna, and Omer Levy. Pick-a-pic: An open dataset of user preferences for text-to-image generation. *Advances in neural information processing systems*, 36:36652–36663, 2023. [6](#), [1](#)

[14] Jiachen Li, Weixi Feng, Wenhui Chen, and William Yang Wang. Reward guided latent consistency distillation. *Transactions on Machine Learning Research*, 2024. [1](#), [3](#), [7](#), [8](#)

[15] Junzhe Li, Yutao Cui, Tao Huang, Yingping Ma, Chun Fan, Miles Yang, and Zhao Zhong. Mixgrpo: Unlocking flow-based grpo efficiency with mixed ode-sde. *arXiv preprint arXiv:2507.21802*, 2025. [1](#), [3](#), [6](#), [7](#), [8](#)

[16] Muyang Li, Yujun Lin, Zhekai Zhang, Tianle Cai, Xiuyu Li, Junxian Guo, Enze Xie, Chenlin Meng, Jun-Yan Zhu, and Song Han. Svdquant: Absorbing outliers by low-rank components for 4-bit diffusion models. *arXiv preprint arXiv:2411.05007*, 2024. [1](#)

[17] Zhanhao Liang, Yuhui Yuan, Shuyang Gu, Bohan Chen, Tiankai Hang, Mingxi Cheng, Ji Li, and Liang Zheng. Aesthetic post-training diffusion models from generic preferences with step-by-step preference optimization. In *Proceedings of the Computer Vision and Pattern Recognition Conference*, pages 13199–13208, 2025. [3](#)

[18] Jie Liu, Gongye Liu, Jiajun Liang, Yangguang Li, Jiaheng Liu, Xintao Wang, Pengfei Wan, Di Zhang, and Wanli Ouyang. Flow-grpo: Training flow matching models via online rl. *Advances in Neural Information Processing Systems*, 2025. [1](#), [3](#), [6](#), [7](#), [8](#)

[19] Wenxuan Liu and Sai Qian Zhang. Hq-dit: Efficient diffusion transformer with fp4 hybrid quantization. *arXiv preprint arXiv:2405.19751*, 2024. [1](#)

[20] Simian Luo, Yiqin Tan, Longbo Huang, Jian Li, and Hang Zhao. Latent consistency models: Synthesizing high-resolution images with few-step inference. *arXiv preprint arXiv:2310.04378*, 2023. [3](#)

[21] Weijian Luo. Diff-instruct++: Training one-step text-to-image generator model to align with human preferences. *Transactions on Machine Learning Research*, 2024. [1](#), [3](#)

[22] Yihong Luo, Tianyang Hu, Weijian Luo, Kenji Kawaguchi, and Jing Tang. Reward-instruct: A reward-centric approach to fast photo-realistic image generation. *Advances in Neural Information Processing Systems*, 2025. [1](#), [2](#), [3](#), [7](#), [8](#)

[23] Zichen Miao, Zhengyuan Yang, Kevin Lin, Ze Wang, Zicheng Liu, Lijuan Wang, and Qiang Qiu. Tuning timestep-distilled diffusion model using pairwise sample optimization. *arXiv preprint arXiv:2410.03190*, 2024. [1](#)

[24] Owen Oertell, Jonathan D Chang, Yiyi Zhang, Kianté Brantley, and Wen Sun. Rl for consistency models: Faster

reward guided text-to-image generation. *arXiv preprint arXiv:2404.03673*, 2024. 1

[25] Yuxi Ren, Xin Xia, Yanzuo Lu, Jiacheng Zhang, Jie Wu, Pan Xie, Xing Wang, and Xuefeng Xiao. Hyper-sd: Trajectory segmented consistency model for efficient image synthesis. *Advances in Neural Information Processing Systems*, 37:117340–117362, 2024. 1, 6, 7

[26] Axel Sauer, Frederic Boesel, Tim Dockhorn, Andreas Blattmann, Patrick Esser, and Robin Rombach. Fast high-resolution image synthesis with latent adversarial diffusion distillation. In *SIGGRAPH Asia 2024 Conference Papers*, pages 1–11, 2024. 3

[27] Zhihong Shao, Peiyi Wang, Qihao Zhu, Runxin Xu, Junxiao Song, Xiao Bi, Haowei Zhang, Mingchuan Zhang, YK Li, Yang Wu, et al. Deepseekmath: Pushing the limits of mathematical reasoning in open language models. *arXiv preprint arXiv:2402.03300*, 2024. 4

[28] Alimama-Creative Team. Flux.1-turbo-alpha, 2024. Accessed: 2025-05-15. 6, 7

[29] Bram Wallace, Meihua Dang, Rafael Rafailov, Linqi Zhou, Aaron Lou, Senthil Purushwalkam, Stefano Ermon, Caiming Xiong, Shafiq Joty, and Nikhil Naik. Diffusion model alignment using direct preference optimization. In *Proceedings of the IEEE/CVF Conference on Computer Vision and Pattern Recognition*, pages 8228–8238, 2024. 3

[30] Fu-Yun Wang, Yunhao Shui, Jingtian Piao, Keqiang Sun, and Hongsheng Li. Diffusion-npo: Negative preference optimization for better preference aligned generation of diffusion models. In *The Thirteenth International Conference on Learning Representations*, 2025. 3

[31] Yibin Wang, Zhimin Li, Yuhang Zang, Yujie Zhou, Jiazi Bu, Chunyu Wang, Qinglin Lu, Cheng Jin, and Jiaqi Wang. Pref-grpo: Pairwise preference reward-based grpo for stable text-to-image reinforcement learning. *arXiv preprint arXiv:2508.20751*, 2025. 3

[32] Yibin Wang, Yuhang Zang, Hao Li, Cheng Jin, and Jiaqi Wang. Unified reward model for multimodal understanding and generation. *arXiv preprint arXiv:2503.05236*, 2025. 2

[33] Xiaoshi Wu, Yiming Hao, Keqiang Sun, Yixiong Chen, Feng Zhu, Rui Zhao, and Hongsheng Li. Human preference score v2: A solid benchmark for evaluating human preferences of text-to-image synthesis. *arXiv preprint arXiv:2306.09341*, 2023. 1

[34] Enze Xie, Junsong Chen, Yuyang Zhao, Jincheng Yu, Ligeng Zhu, Chengyue Wu, Yujun Lin, Zhekai Zhang, Muyang Li, Junyu Chen, et al. Sana 1.5: Efficient scaling of training-time and inference-time compute in linear diffusion transformer. *arXiv preprint arXiv:2501.18427*, 2025. 1, 6

[35] Jiazheng Xu, Xiao Liu, Yuchen Wu, Yuxuan Tong, Qinkai Li, Ming Ding, Jie Tang, and Yuxiao Dong. Imagereward: Learning and evaluating human preferences for text-to-image generation. *Advances in Neural Information Processing Systems*, 36:15903–15935, 2023. 1

[36] Shuchen Xue, Chongjian Ge, Shilong Zhang, Yichen Li, and Zhi-Ming Ma. Advantage weighted matching: Aligning rl with pretraining in diffusion models. *arXiv preprint arXiv:2509.25050*, 2025. 6

[37] Zeyue Xue, Jie Wu, Yu Gao, Fangyuan Kong, Lingting Zhu, Mengzhao Chen, Zhiheng Liu, Wei Liu, Qiushan Guo, Weilin Huang, et al. Dancegrpo: Unleashing grpo on visual generation. *arXiv preprint arXiv:2505.07818*, 2025. 1, 3, 6, 7, 8

[38] Tianwei Yin, Michaël Gharbi, Richard Zhang, Eli Shechtman, Fredo Durand, William T Freeman, and Taesung Park. One-step diffusion with distribution matching distillation. In *Proceedings of the IEEE/CVF conference on computer vision and pattern recognition*, pages 6613–6623, 2024. 3

[39] Benjamin Yu, Jackie Liu, and Justin Cui. Smart-grpo: Smartly sampling noise for efficient rl of flow-matching models. *arXiv preprint arXiv:2510.02654*, 2025. 1

[40] Tao Zhang, Cheng Da, Kun Ding, Huan Yang, Kun Jin, Yan Li, Tingting Gao, Di Zhang, Shiming Xiang, and Chun-hong Pan. Diffusion model as a noise-aware latent reward model for step-level preference optimization. *arXiv preprint arXiv:2502.01051*, 2025. 3

[41] Tianchen Zhao, Tongcheng Fang, Haofeng Huang, Enshu Liu, Rui Wan, Widya Dewi Soedarmadji, Shiyao Li, Zinan Lin, Guohao Dai, Shengen Yan, et al. Vedit-q: Efficient and accurate quantization of diffusion transformers for image and video generation. *arXiv preprint arXiv:2406.02540*, 2024. 1

[42] Yujie Zhou, Pengyang Ling, Jiazi Bu, Yibin Wang, Yuhang Zang, Jiaqi Wang, Li Niu, and Guangtao Zhai. G2rpo: Granular grpo for precise reward in flow models. *arXiv preprint arXiv:2510.01982*, 2025. 1

Know Your Step: Faster and Better Alignment for Flow Matching Models via Step-aware Advantages

Supplementary Material

6. Extended Experimental Results

6.1. Additional Qualitative Results

Figure 5 shows the qualitatively compare TAFS-GRPO with Flux.1-Dev, Flux.1-Schnell and Flux-Hyper on the composition image generation task. The results of TAFS-GRPO show significant improvements in object-focused tasks such as object presence, counting, and spatial relationships.

6.2. Reward Model Sensitivity Analysis

Reward Model	Pick Score \uparrow	CLIP \uparrow	HPS-v2.1 \uparrow	Unified R \uparrow
CLIP-only	22.01	27.92	0.312	3.421
PickScore-only	22.58	26.74	0.298	3.398
Combined	22.46	27.68	0.353	3.511

Table 6. Experiment on reward sensitivity with Flux.1-dev base model and tested under 8 inference steps.

We conducted a sensitivity analysis to evaluate the impact of different reward model configurations during training. The results in Table 6 indicate that using a single reward model leads to noticeable performance degradation in certain out-of-domain metrics. In contrast, the combined reward model achieved the best overall balance across both in-domain and out-of-domain evaluation metrics. These findings suggest that multi-reward integration enhances model robustness and effectively mitigates overfitting to any single metric.

6.3. Analysis of Intermediate Reward Validity

A key premise of TAFS-GRPO is that the one-step clean estimates x_0^n derived from noisy states $x_{T-n\tau}$ contain sufficient semantic content to provide valid reward signals. To validate this, we computed the Pearson correlation coefficient between the reward scores of the intermediate estimates and the final generated image across 1,000 training prompts. As shown in Table 7, even the early step reward R^2 estimates show a strong positive correlation ($r > 0.65$) with the final quality. This indicates that although early estimates may lack high-frequency details, they successfully capture the global semantic structure (e.g., object presence, composition) required by reward models like CLIP and PickScore. This validates the use of dense supervision, as the signal provided by early steps guide the model in a direction consistent with the final objective.

Step Reward	PickScore (r)	CLIP Score (r)
R^2 with R^4	0.68	0.72
R^3 with R^4	0.84	0.88

Table 7. Correlation between intermediate step rewards and final step rewards.

7. Experiment Setup Details

7.1. Hyperparameters Settings

We use LoRA with $\alpha = 64$ and $r = 32$ on both Flux.1-dev and SD3.5-M base models. For each iteration, we use a group size of 48, a batch size of 3 per GPU and total batch size of 24 on all tasks. We train our model using 8 NVIDIA H100 GPUs for 1500 iterations to ensure convergence.

7.2. Details on Evaluation Metrics

We introduce further details of the metrics used in the composition image generation task and human preference alignment task.

GenEval Score. GenEval [6] score is an automated evaluation metric designed to assess text-to-image models on fine-grained, object-focused tasks such as object presence, counting, spatial relationships, color accuracy, and attribute binding.

Pick Score. Pick score [13] is a CLIP-based scoring function trained on the Pick-a-Pic dataset, a large, open collection of real user preferences for text-to-image generation. Its primary purpose is to predict human preferences by evaluating how well a generated image aligns with a given text prompt, which maximizes the probability that a preferred image is ranked higher than a non-preferred one.

CLIP Score. The CLIP Score [9] is a reference-free evaluation metric that quantifies the semantic alignment between a generated image and its corresponding text prompt. It leverages the pre-trained CLIP model, which projects both images and text into a shared embedding space. The score is computed as the cosine similarity between the image embedding and the text embedding, measuring how closely the visual content matches the textual description in a high-level semantic sense.

HPS-v2.1 Score. Human Preference Score v2.1 [33] is a metric designed to evaluate the alignment of text-to-image generative models with human aesthetic preferences.

ImageReward ImageReward [35] is a general-purpose text-to-image human preference reward model designed to effectively encode human preferences for images gener-

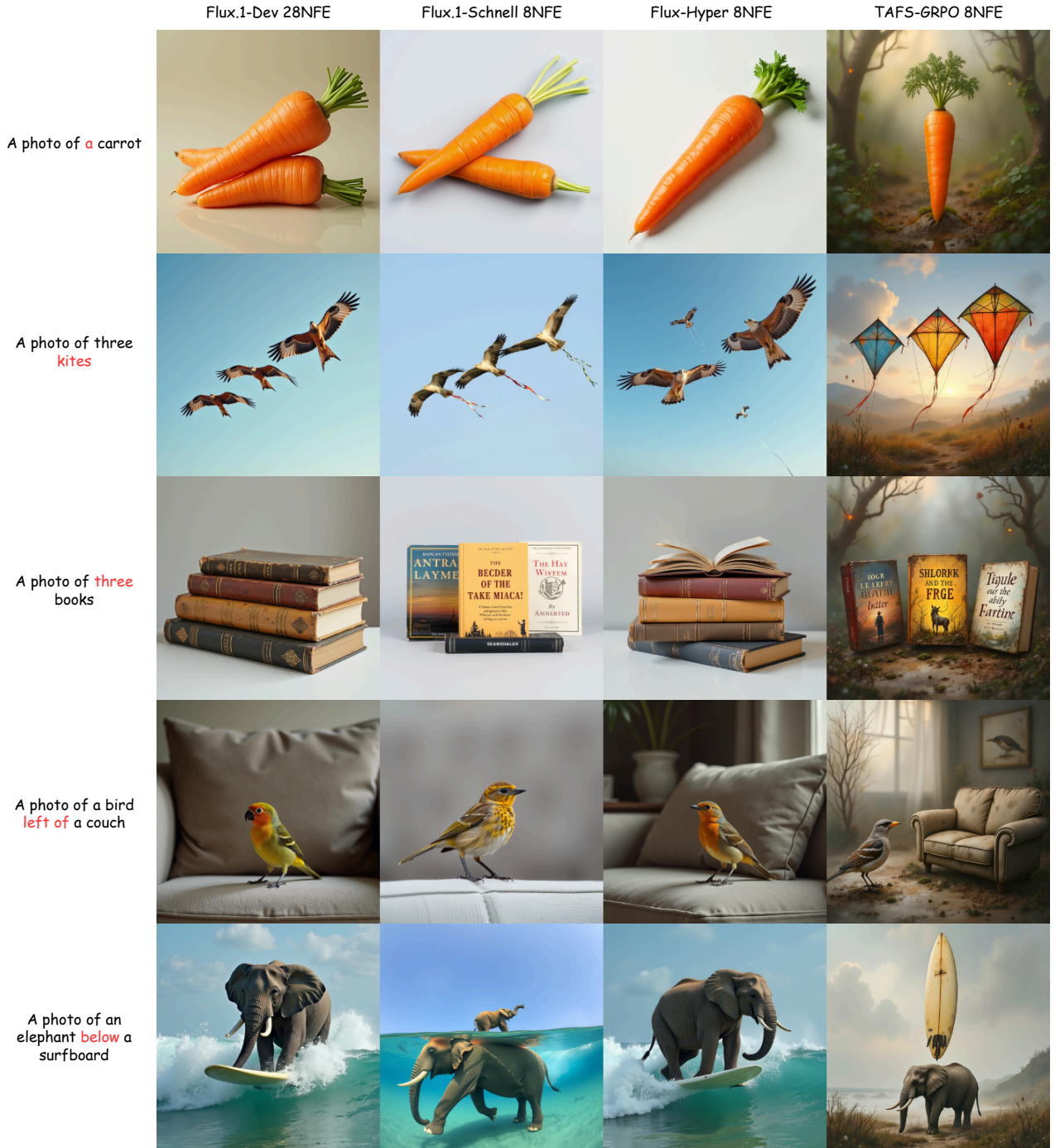


Figure 5. Qualitative comparison of generations on the composition image generation task from 28 sampling steps of Flux.1-Dev, and 8 sampling steps of Flux.1-Schnell, Flux-Hyper, and the proposed TAFS-GRPO.

ated from text prompts. Trained on a large-scale dataset of 137,000 expert comparisons collected through a systematic annotation pipeline involving rating and ranking.

Unified Reward. The Unified Reward Model [32] is designed to assess both multimodal understanding and gener-

ation tasks. It overcomes the limitations of traditional, task-specific reward models by leveraging joint learning across diverse visual tasks, which creates a synergistic effect where improvements in one domain (e.g., image understanding) enhance performance in another (e.g., image assessment).